

Computational Studies on Phosphodiesterase-5 Inhibitors to Design Novel Lead Compounds for the Treatment of Erectile Dysfunction

L. Jayashankar *, Prof. B. Syama Sundar

Department of Pharmacy, Acharya Nagarjuna University, Guntur – 522510, Andrapradesh, India

Abstract:

2D and 3D Quantitative Structural Activity Relationship studies using Molecular Field Analysis (MFA) and Receptor surface Analysis (RSA) methods along with pharmacophore hypothesis using Catalyst version 4.7 were performed on a series of Phosphodiesterase 5 (PDE-5) inhibitors. The best equations with training set consisting 41 molecules, produced r^2 value of 0.788 and r^2_{cv} value of 0.618 in 2D-model and r^2 value of 0.844 and r^2_{cv} value of 0.810 in MFA-model and r^2 value of 0.853 & r^2_{cv} of 0.799 in the RSA-model. Pharmacophore models were generated using 20 molecules as training set. The best quantitative pharmacophore model consists of one hydrogen bond acceptor, one hydrophobic aliphatic and two ring aromatic features. We have constructed a large set of 75 test compounds, and conformational studies were done as described earlier. The estimated activities were scored using hypothesis 1 as the pharmacophore. Out of 25 highly active compounds (<50nM), 15 were accurately predicted as highly active and the remaining were all predicted as moderately active. Out of the 33 moderately active compounds (50-1000nM), 4 were predicted as inactive and one was predicted highly active. Out of the 16 inactive compounds (>1000nM), 8 were predicted to be inactive and 8 were predicted to be moderately active

Keywords: 3D QSAR, CAT B, MFA, RSA, Catalyst, Pharmacophore.

Introduction:

A phosphodiesterase is an enzyme that catalyzes the hydrolysis of phosphodiester bonds, for instance a bond in a molecule of cyclic AMP or cyclic GMP. It plays a role in signal transduction by regulating the intracellular concentration of cyclic nucleotides. This phosphodiesterase catalyzes the specific hydrolysis of cGMP to 5'-GMP. Human phosphodiesterase 5 is responsible for the degradation of cyclic GMP in the corpus cavernosum. It is well known target for erectile dysfunction and pulmonary hypertension. The wide-ranging functions of this enzyme therefore make it an attractive drug discovery target [1 and 2]. We have performed Pharmacophore and QSAR studies for developing novel PDE-5 inhibitors [3-8] using the Catalyst 4.7 and Cerius2 program suite respectively [9-29]. QSAR equations has been generated for 51 PDE-5 inhibitors employing Molecular Field Analysis (MFA) as well as Receptor surface Analysis (RSA) using Genetic function approximation (GFA) as regression method. We intend to employ the pharmacophore information to execute 3D-database virtual screening to discover reliable and potential Novel Lead structure against PDE-5 inhibitors for treatment of erectile

dysfunction.

Materials and Methods:

All molecular modeling works were carried out by using DISCOVERY STUDIO 2.5 software package (Accelrys, San Diego, CAUSA). [All the catalyst functions are in-built modules of Discovery Studio].

Experimental work:

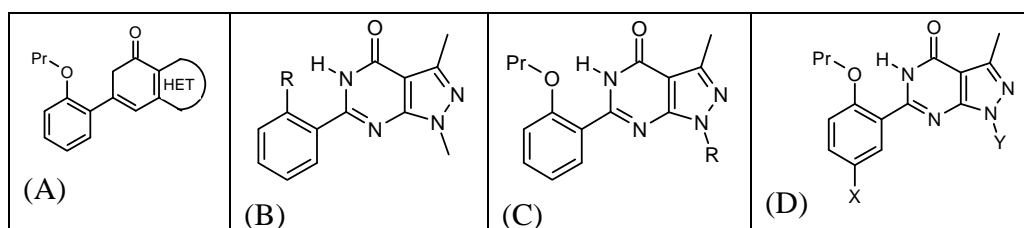
40 molecules forming the training set were used to generate the QSAR equation. For MFA studies molecular field was created using proton and methyl groups as probes, which represent electrostatic and steric fields respectively. For RSA studies chemical properties namely charge, electrostatic potential, hydrogen bonding propensity and hydrophobicity associated with each surface point were calculated. For generating equations, only 10% of the total descriptors whose variance was highest were considered for further analysis. Regression analysis was carried out using G/PLS method consisting of over 50,000 generations with a population size of 100 (Table. 2.1 and 2.2)

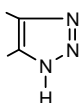
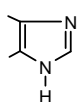
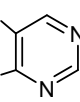
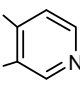
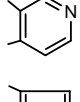
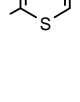
Catalyst version 4.7 was used to generate Pharmacophore models. 20 molecules forming the training set were used to generate Hypogen hypothesis.

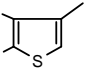
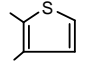
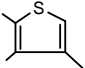
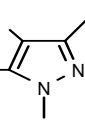
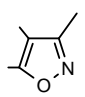
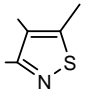
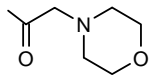
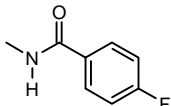
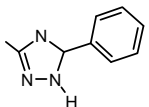
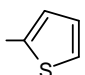
Table 1: Statistical details of 2D, MFA, & RSA analysis

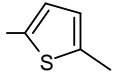
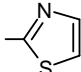
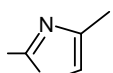
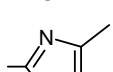
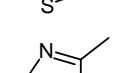
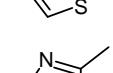
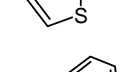
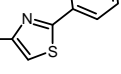
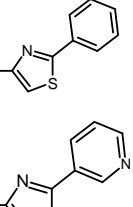
| Serial No. | Statistics | 2D | MFA | RSA |
|------------|------------|--------|-------|-------|
| 01 | R | 0.888 | 0.919 | 0.923 |
| 02 | r^2 | 0.788 | 0.844 | 0.853 |
| 03 | xvr^2 | 0.618 | 0.810 | 0.799 |
| 04 | Bsr^2 | 0.655 | 0.837 | 0.846 |
| 05 | PRESS | 10.490 | 5.227 | 5.513 |

a. MFA: Molecular Field Analysis, b. RSA: Receptor surface Analysis, c. R 2: Regression Analysis, d. XVR2: Cross validated R2, e. PRESS: Predicted sum of squared residuals.

Table 2.1: Training Set with Experimental and Predicted Activity

| Compound No. | Scaffold class | HET/R/X | Y | Experimental | | Predicted | | |
|--------------|----------------|---|---|---------------------|-------------------|-----------|--------|--------|
| | | | | IC ₅₀ nM | pIC ₅₀ | 2D | MFA | RSA |
| 1 | A |  | | 200 | -2.300 | -2.465 | -2.219 | -2.492 |
| 2 | A |  | | 80 | -1.900 | -2.174 | -2.321 | -2.354 |
| 3 | A |  | | 300 | -2.480 | -2.107 | -2.439 | -2.535 |
| 4 | A |  | | 70 | -1.850 | -1.732 | -1.898 | -1.853 |
| 5 | A |  | | 50 | -1.700 | -1.814 | -1.886 | -1.927 |
| 6 | A |  | | 100 | -2.000 | -2.118 | -2.306 | -1.921 |

| | | | | | | | | |
|----|---|---|----|-----|--------|--------|--------|--------|
| 7 | A |  | | 60 | -1.780 | -1.695 | -1.586 | -1.482 |
| 8 | A |  | | 50 | -1.700 | -2.023 | -1.983 | -1.868 |
| 9 | A |  | | 80 | -1.900 | -1.622 | -1.985 | -1.570 |
| 10 | A |  | | 8 | -0.900 | -1.367 | -1.249 | -0.920 |
| 11 | A |  | | 100 | -2.000 | -2.001 | -1.856 | -2.264 |
| 12 | A |  | | 30 | -1.480 | -1.887 | -1.836 | -1.840 |
| 13 | B | O-Isopropyl | | 40 | -1.600 | -1.109 | -1.249 | -1.243 |
| 14 | C | Butyl | | 6 | -0.780 | -0.776 | -0.956 | -0.868 |
| 15 | C | Tertiary butyl | | 20 | -1.300 | -0.846 | -0.957 | -1.119 |
| 16 | C | CH ₂ CF ₃ | | 7 | -0.850 | -0.735 | -0.956 | -1.014 |
| 17 | D |  | Me | 4 | -0.600 | -0.823 | -0.550 | -0.358 |
| 18 | D | NO ₂ | Me | 4 | -0.600 | -0.983 | -0.549 | -0.597 |
| 19 | D | NH ₂ | Et | 7 | -0.850 | -0.678 | -0.877 | -0.692 |
| 20 | D | N(Me) ₂ | Me | 5 | -0.700 | -0.918 | -0.550 | -0.380 |
| 21 | D | N(Me) ₂ | Et | 4 | -0.600 | -0.928 | -0.550 | -0.725 |
| 22 | D | NHSO ₂ Me | Me | 3 | -0.480 | -0.334 | -0.551 | -0.368 |
| 23 | D | NHSO ₂ Me | Et | 4 | -0.600 | -0.234 | -0.340 | -0.528 |
| 24 | D | NHCOMe | Et | 2 | -0.300 | -0.709 | -0.257 | -0.503 |
| 25 | D |  | Me | 2 | -0.300 | -0.443 | -0.550 | -0.430 |
| 26 | D | NHCOOMe | Me | 2 | -0.300 | -0.747 | -0.550 | -0.477 |
| 27 | D | NHCONH ₂ | Me | 2 | -0.300 | -0.849 | -0.550 | -0.577 |
| 28 | D | NHCONHEt | Me | 3 | -0.480 | -0.545 | -0.550 | -0.523 |
| 29 | D | NHCSNHEt | Me | 3 | -0.480 | -0.345 | -0.550 | -0.545 |
| 30 | D | NHCSNHCOOEt | Me | 2 | -0.300 | -0.152 | -0.550 | -0.645 |
| 31 | D |  | Me | 20 | -1.300 | -0.387 | -0.550 | -0.372 |
| 32 | D |  | Me | 5 | -0.700 | -0.769 | -0.550 | -0.732 |

| | | | | | | | | |
|----|---|---|----|-----|--------|--------|--------|--------|
| 33 | D |  | Me | 4 | -0.600 | -0.661 | -0.550 | -0.396 |
| 34 | D |  | Me | 3 | -0.480 | -0.882 | -0.550 | -0.538 |
| 35 | D |  | Me | 2.5 | -0.400 | -0.537 | -0.551 | -0.519 |
| 36 | D |  | Et | 2 | -0.300 | -0.412 | -0.257 | -0.468 |
| 37 | D |  | Me | 2.5 | -0.400 | -0.513 | -0.551 | -0.566 |
| 38 | D |  | Et | 3 | -0.480 | -0.454 | -0.238 | -0.496 |
| 39 | D |  | Me | 2.5 | -0.400 | -0.322 | -0.550 | -0.568 |
| 40 | D |  | Et | 3 | -0.480 | -0.316 | -0.257 | -0.440 |
| 41 | D |  | Et | 2 | -0.300 | -0.233 | -0.257 | -0.437 |

Et denotes Ethyl, Me denotes Methyl, Pr denotes Propyl

All structures were built and minimized within the Catalyst software package, and conformational analysis of each molecule was implemented using the poling algorithm. Hypotheses were generated from a collection of conformational models of compounds spanning activities of 4-5 orders of magnitude.

Results and discussion:

Molecular field analysis (MFA)

2D equation:

$$\text{Activity} = 32.1973 + 0.11033 * \text{“MW”} + 0.036525 * \text{“Area”} - 0.163124 * \text{“VM”} - 31.2449 * \text{“Density”}$$

The term MW +0.11033 denotes the molecular weight and the term Vm - 0.163124 denotes the molecular volume

MFA equation:

$$\text{Activity} = -2.57287 + 0.009541 * \text{“CH3/549”} + 0.022934 * \text{“CH3/276”} + 0.020199 * \text{“CH3/534”} + 0.02451 * \text{“CH3/771”}$$

MFA equation that for the probe point of CH3 at position 534 in MFA grid indicates bulky groups are favored to decrease the activity. Stereo view of MFA grid is shown in Fig. 1

Receptor surface analysis (RSA)

RSA equation:

$$\text{Activity}_1 = -1.08728 + 1.35507 * \text{“VDW/3789”} - 2.1011 * \text{“ELE/2083”} + 3.04312 * \text{“ELE/2937”} - 1.57952 * \text{“VDW/3091”}$$

The term ELE/2083 in the RSA equation indicates electronegative groups are favored to enhance the activity.

Table 2.2: Test Set with Experimental and Predicted Activity

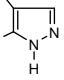
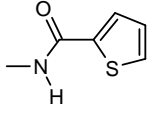
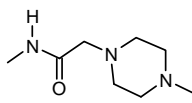
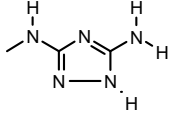
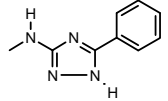
| Compound No. | Scaffold class | HET/R/X | Y | Experimental | | Predicted | | |
|--------------|----------------|---|----|-----------------------|-------------------|-----------|--------|--------|
| | | | | IC ₅₀ (nM) | pIC ₅₀ | 2D | MFA | RSA |
| 1 | A |  | - | 200 | -2.18 | -2.025 | -2.110 | -1.781 |
| 2 | B | OEt | - | 30 | -1.48 | -1.215 | -1.249 | -0.995 |
| 3 | B | SPr | - | 2000 | -3.300 | -2.465 | -2.219 | -2.492 |
| 4 | C | Et | - | 2 | -0.300 | -0.806 | -0.956 | -0.871 |
| 5 | C | Benzyl | - | 70 | -1.850 | -0.960 | -1.251 | -1.870 |
| 6 | D | NH ₂ | Me | 10 | -1.000 | -0.818 | -1.170 | -0.683 |
| 7 | D |  | Me | 1.5 | -0.180 | -0.532 | -0.550 | -0.437 |
| 8 | D |  | Me | 3.5 | -0.540 | -0.761 | -0.55 | -0.491 |
| 9 | D |  | Me | 5 | -0.700 | -0.401 | -0.550 | -0.878 |
| 10 | D |  | Et | 20 | -0.230 | -0.402 | -0.257 | -0.356 |

Table 3: 10 Pharmacophore Hypotheses Generated Using 20 Training Set Molecules

| Hypothesis No ^a | Total Cost | Cost Difference (Null cost – Total cost) | Error Cost | RMS | Correlation (r) | Features ^b |
|----------------------------|------------|--|------------|-------|-----------------|-----------------------|
| 01 | 100.626 | 49.312 | 77.643 | 1.018 | 0.940 | A H R R |
| 02 | 102.325 | 47.613 | 81.886 | 1.208 | 0.909 | A H H R |
| 03 | 102.822 | 47.116 | 81.212 | 1.180 | 0.915 | A H R R |
| 04 | 103.198 | 46.74 | 82.407 | 1.230 | 0.906 | A H R R |
| 05 | 103.805 | 46.133 | 83.487 | 1.273 | 0.898 | A H H R |

| | | | | | | |
|----|---------|--------|--------|-------|-------|-----------|
| 06 | 103.839 | 46.099 | 83.977 | 1.292 | 0.894 | A H H R |
| 07 | 104.005 | 45.933 | 84.916 | 1.328 | 0.887 | A H H R |
| 08 | 104.93 | 45.008 | 84.707 | 1.320 | 0.889 | A H H R |
| 09 | 104.954 | 44.984 | 86.295 | 1.379 | 0.877 | A H H H R |
| 10 | 105.385 | 44.553 | 83.560 | 1.276 | 0.900 | A A H R |

a. Null cost = 149.938, Fixed cost = 85.9304, Configuration = 17.5334, Weight = 1.963, b. A, Hydrogen Bond Acceptor; H, Hydrophobic Aliphatic; R, Ring Aromatic.

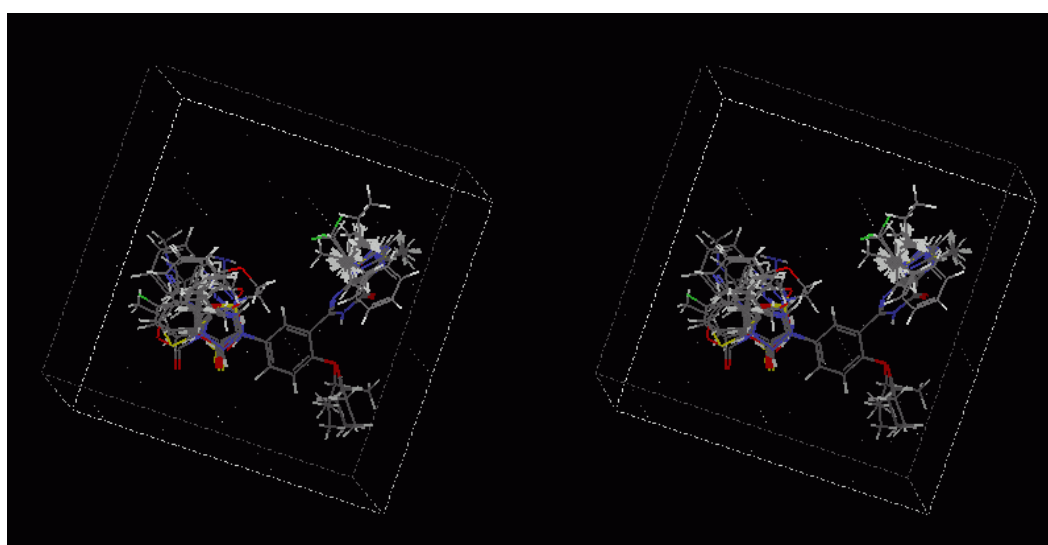


Fig 1: Stereo view of rectangular molecular field surrounding aligned molecules. Some of the field descriptors, which are involved in the equation, are indicated. Correlation of MFA (0.844)

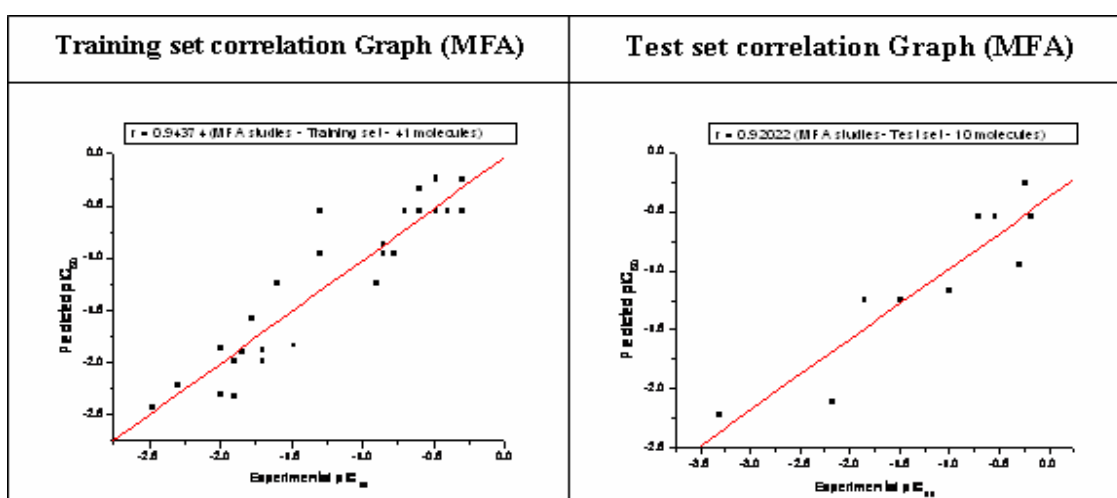


Fig 2: Stereo view of the receptor surface which represents the vitural active site. Some of the RSA descriptors that constitute the equation are labeled. Correlation of RSA (0.853).

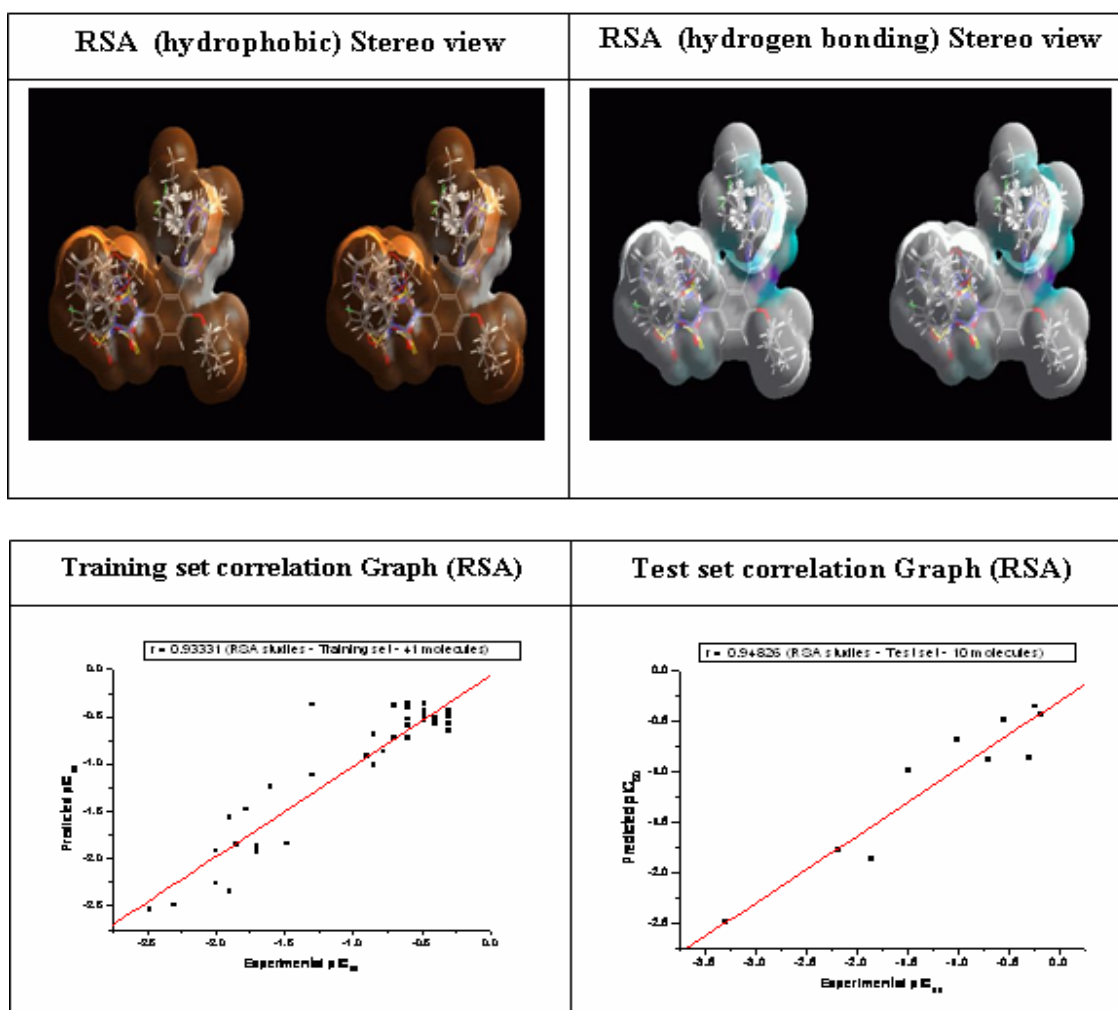
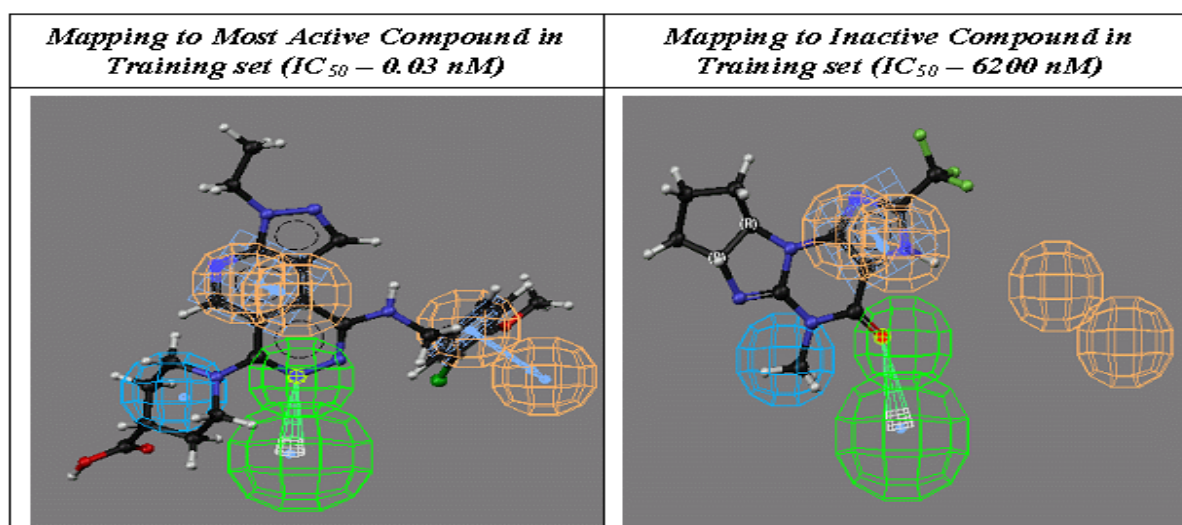
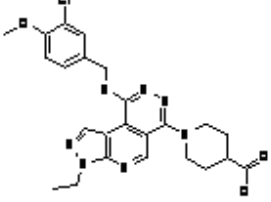
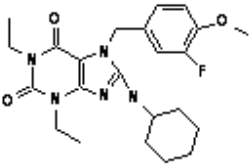
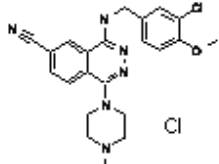
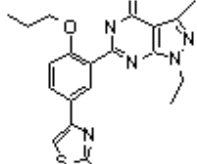
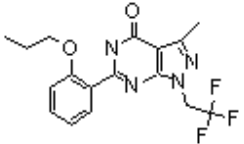
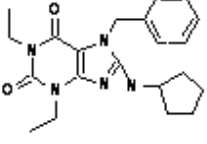
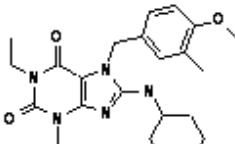
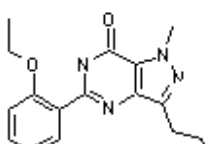
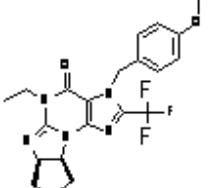
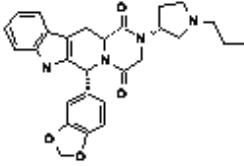
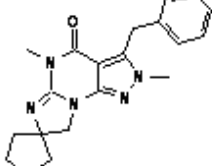
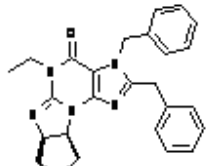
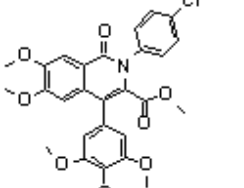
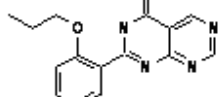
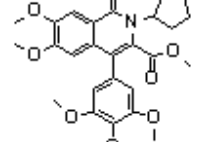
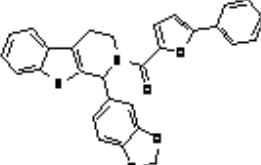
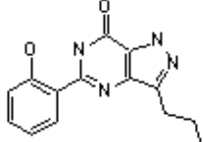
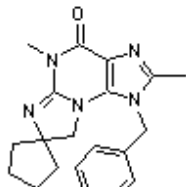
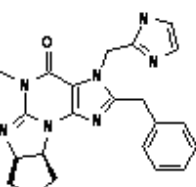
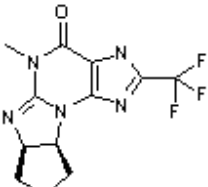


Fig 3: Pharmacophore Mapping



Chemical Structures of the 20 Training Set Molecules Applied to HypoGen Pharmacophore Generation (PDE-5 Activities Are Given as IC_{50} Values)

20 Training set molecules used for validation studies

| | | | |
|---|---|--|---|
|  |  |  |  |
| 1, IC ₅₀ 0.03 nM | 2, IC ₅₀ 0.3 nM | 3, IC ₅₀ 0.95 nM | 4, IC ₅₀ 3 nM |
|  |  |  |  |
| 5, IC ₅₀ 7 nM | 6, IC ₅₀ 10 nM | 7, IC ₅₀ 19 nM | 8, IC ₅₀ 27 nM |
|  |  |  |  |
| 9, IC ₅₀ 48 nM | 10, IC ₅₀ 57 nM | 11, IC ₅₀ 75 nM | 12, IC ₅₀ 130 nM |
|  |  |  |  |
| 13, IC ₅₀ 170 nM | 14, IC ₅₀ 300 nM | 15, IC ₅₀ 580 nM | 16, IC ₅₀ 750 nM |
|  |  |  |  |
| 17, IC ₅₀ 1000 nM | 18, IC ₅₀ 2900 nM | 19, IC ₅₀ 4000 nM | 20, IC ₅₀ 6200 nM |

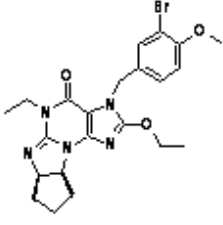
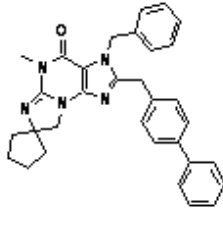
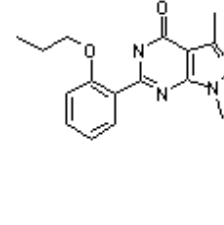
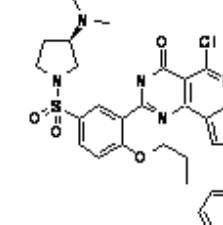
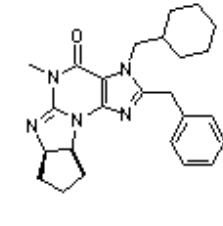
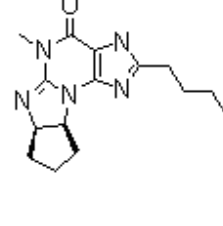
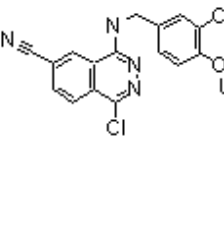
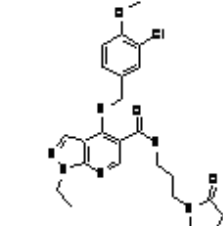
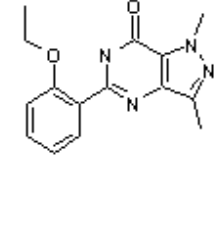
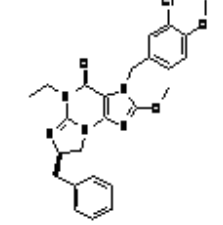
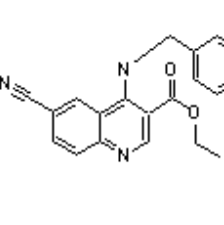
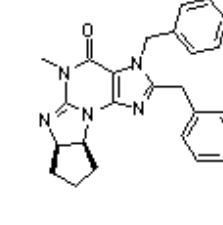
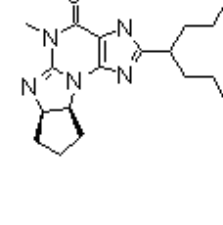
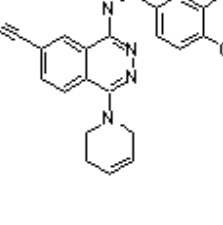
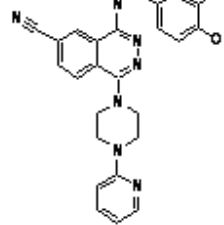
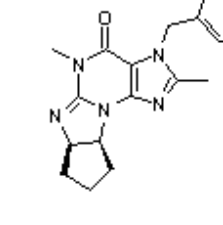
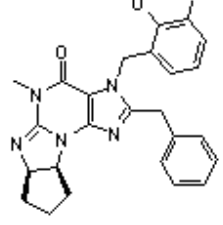
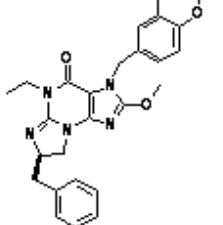
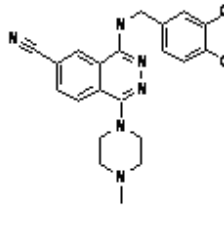
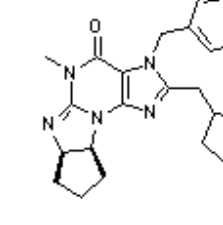
RSA Model with Hydrophobic property and Hydrogen bonding mapped onto it is shown in Fig. 2.

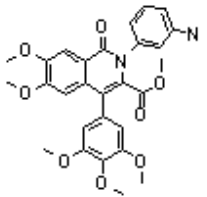
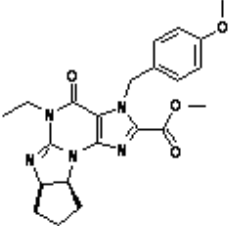
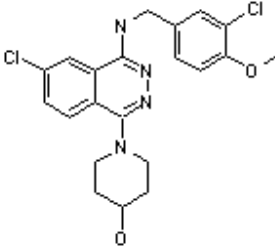
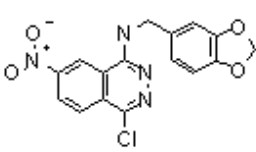
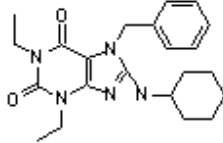
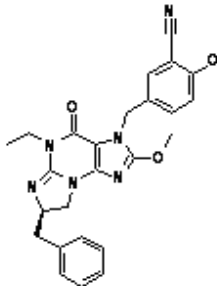
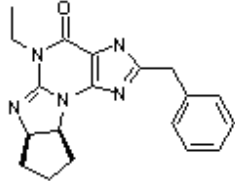
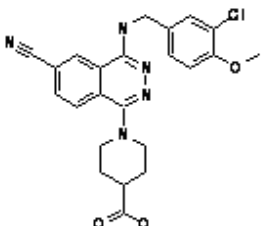
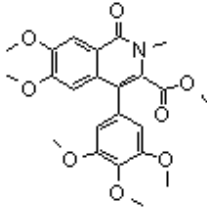
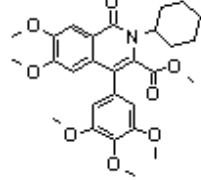
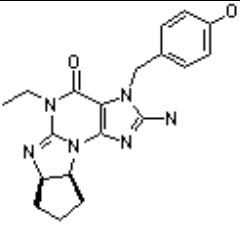
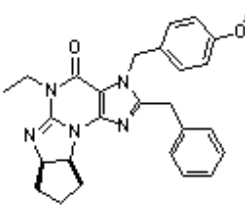
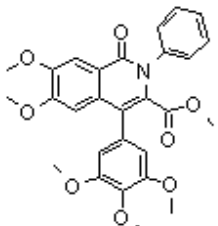
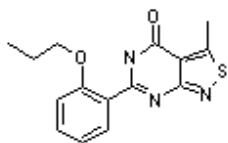
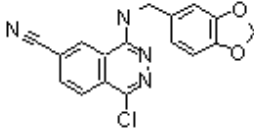
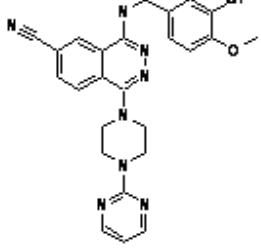
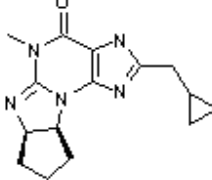
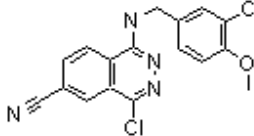
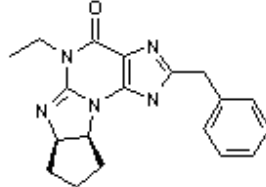
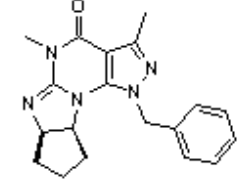
Statistical details of 2D, MFA, & RSA analysis were given in Table. 1

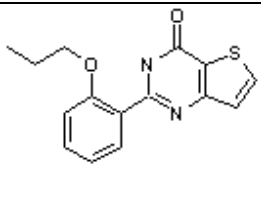
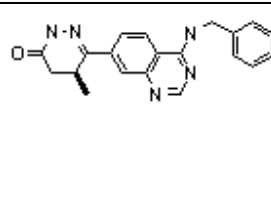
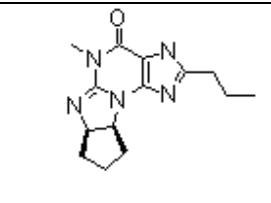
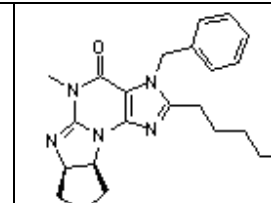
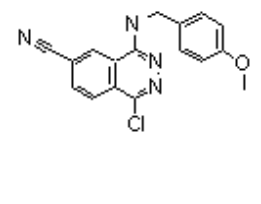
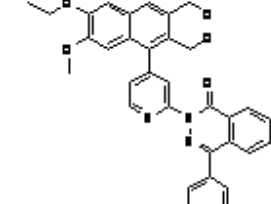
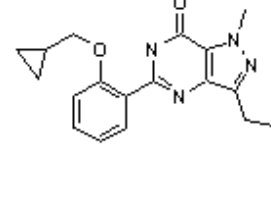
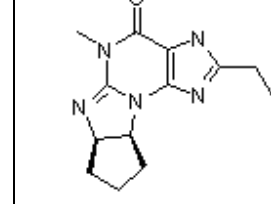
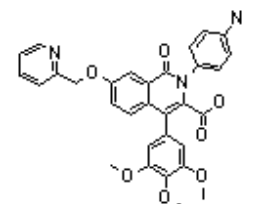
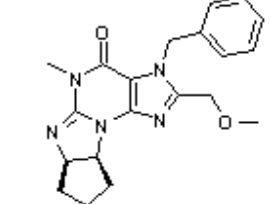
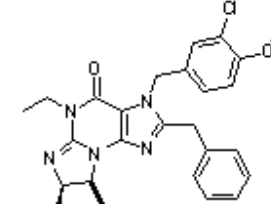
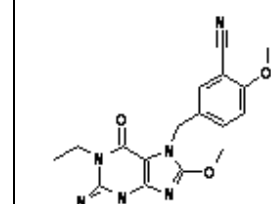
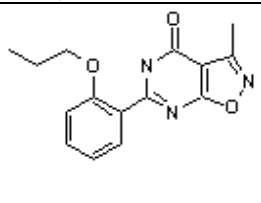
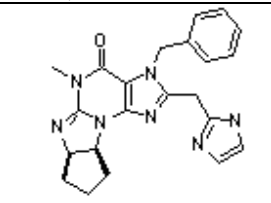
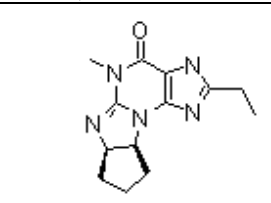
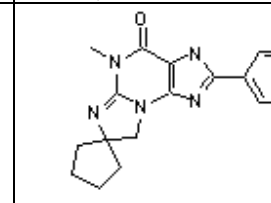
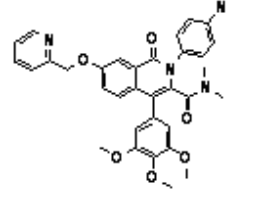
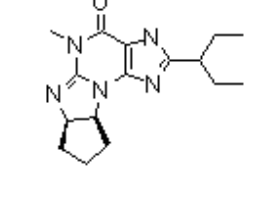
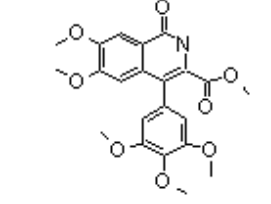
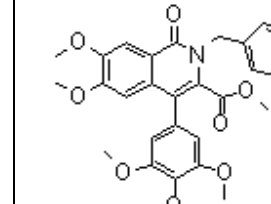
Pharmacophore Hypothesis Generation

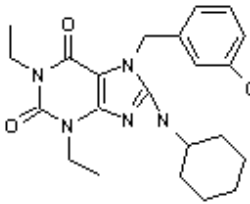
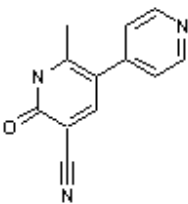
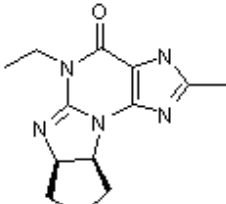
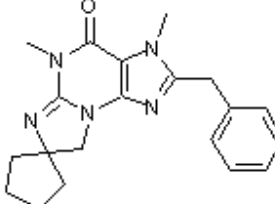
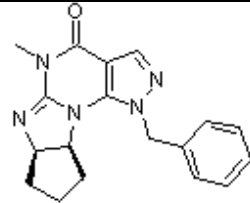
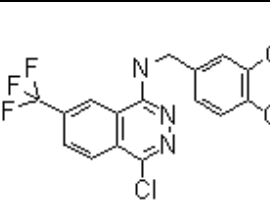
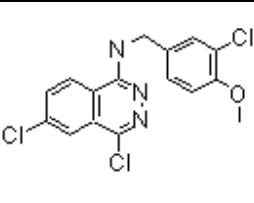
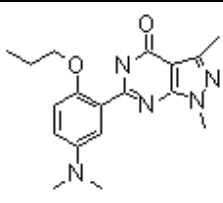
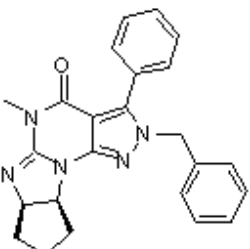
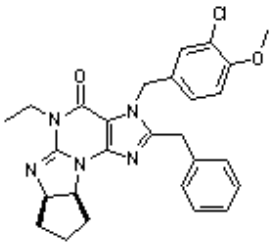
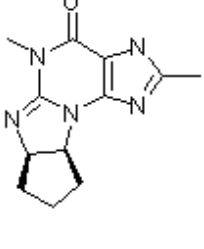
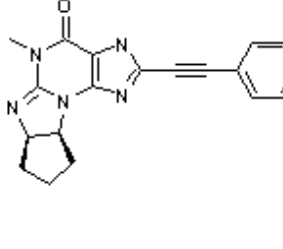
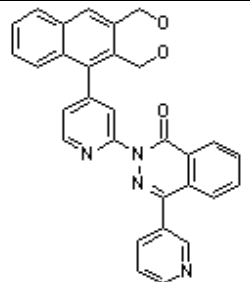
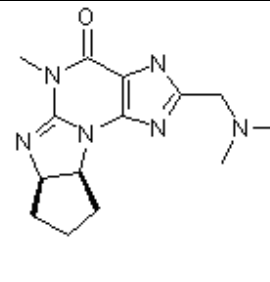
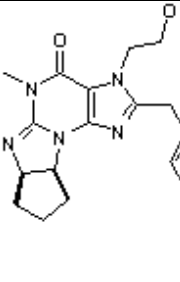
Training set consists of 20 compounds tested against PDE-5 was used to develop Pharmacophore hypotheses.

75 Test set molecules used for validation studies

| | | | |
|---|---|--|---|
|  |  |  |  |
| 1, IC ₅₀ 1.6 nM | 2, IC ₅₀ 1.6 nM | 3, IC ₅₀ 1.9 nM | 4, IC ₅₀ 2.2 nM |
|  |  |  |  |
| 5, IC ₅₀ 3.1 nM | 6, IC ₅₀ 4 nM | 7, IC ₅₀ 4.4 nM | 8, IC ₅₀ 5.3 nM |
|  |  |  |  |
| 9, IC ₅₀ 5.4 nM | 10, IC ₅₀ 6.8 nM | 11, IC ₅₀ 8 nM | 12, IC ₅₀ 11 nM |
|  |  |  |  |
| 13, IC ₅₀ 11 nM | 14, IC ₅₀ 12 nM | 15, IC ₅₀ 13 nM | 16, IC ₅₀ 19 nM |
|  |  |  |  |
| 17, IC ₅₀ 19 nM | 18, IC ₅₀ 20 nM | 19, IC ₅₀ 22 nM | 20, IC ₅₀ 30 nM |

| | | | |
|---|---|--|---|
|  |  |  |  |
| 21, IC ₅₀ 30 nM | 22, IC ₅₀ 39 nM | 23, IC ₅₀ 43 nM | 24, IC ₅₀ 49 nM |
|  |  |  |  |
| 25, IC ₅₀ 50 nM | 26, IC ₅₀ 58 nM | 27, IC ₅₀ 63 nM | 28, IC ₅₀ 100 nM |
|  |  |  |  |
| 29, IC ₅₀ 100 nM | 30, IC ₅₀ 100 nM | 31, IC ₅₀ 100 nM | 32, IC ₅₀ 110 nM |
|  |  |  |  |
| 33, IC ₅₀ 140 nM | 34, IC ₅₀ 140 nM | 35, IC ₅₀ 140 nM | 36, IC ₅₀ 150 nM |
|  |  |  |  |
| 37, IC ₅₀ 160 nM | 38, IC ₅₀ 180 nM | 39, IC ₅₀ 200 nM | 40, IC ₅₀ 200 nM |

| | | | |
|---|---|--|---|
|  |  |  |  |
| 41, IC ₅₀ 200 nM | 42, IC ₅₀ 225 nM | 43, IC ₅₀ 230 nM | 44, IC ₅₀ 230 nM |
|  |  |  |  |
| 45, IC ₅₀ 2250 nM | 46, IC ₅₀ 275 nM | 47, IC ₅₀ 330 nM | 48, IC ₅₀ 380 nM |
|  |  |  |  |
| 49, IC ₅₀ 610 nM | 50, IC ₅₀ 800 nM | 51, IC ₅₀ 800 nM | 52, IC ₅₀ 800 nM |
|  |  |  |  |
| 53, IC ₅₀ 810 nM | 54, IC ₅₀ 900 nM | 55, IC ₅₀ 960 nM | 56, IC ₅₀ 1000 nM |
|  |  |  |  |
| 57, IC ₅₀ 1000 nM | 58, IC ₅₀ 1000 nM | 59, IC ₅₀ 1000 nM | 60, IC ₅₀ 1200 nM |

| | | | |
|---|---|--|--|
|  |  |  |  |
| 61, IC50 1400 nM | 62, IC50 01500 nM | 63, IC50 1900 nM | 64, IC50 2100 nM |
|  |  |  |  |
| 65, IC50 2100 nM | 66, IC50 2400 nM | 67, IC50 2900 nM | 68, IC50 3100 nM |
|  |  |  |  |
| 69, IC50 3300 nM | 70, IC50 4500 nM | 71, IC50 5000 nM | 72, IC50 6000 nM |
|  |  |  | |
| 73, IC50 7500 nM | 74, IC50 10000 nM | 75, IC50 1000 nM | |

A total of 10 hypotheses were generated and its different cost values, correlation coefficients (r), RMS deviations, and pharmacophore feature definitions are listed in Table 3. For the training set the accuracy in predicting active and inactive compounds was 90%. The selected pharmacophore hypothesis yielded a RMS deviation of 1.018 and a correlation coefficient of 0.940 with a cost difference of 49.312. The best

pharmacophore model was validated on 75 test molecules to give correlation value of 0.898. For the test set, the accuracy in predicting active compounds was greater than 10%, while 14% and 6% representing both false positive and negative respectively. The mapping of Hypothesis1 model onto an active and inactive training set Compound (IC50 = 0.03 nM and 6200 nM respectively) is shown in Fig 3.

Conclusion:

The results from these QSAR analyses provide a useful insight into the structural and electrostatic requirements for binding of a ligand to the PDE-5 receptor and these derivatives 2D, MFA and RSA could provides us useful information for developing extremely potent ligands leading to potential PDE-5 inhibitors. In 2D QSAR, the shape of the molecule is more important in relation to biological activity. In 3D QSAR, MFA studies shows that steric buck groups seem to play a crucial role on preferred locations on the analogs, such that it improves the activity and RSA shows the role of vander waals and electrostatic interactions. Further, the knowledge of this four-feature pharmacophore hypothesis for PDE-5 inhibitors can be very useful for virtual screening to design more potent lead moieties for the treatment of various types of Erectile Dysfunction.

Acknowledgement:

We sincerely thank Sai BioSciences Research Institute (SBRI), Chennai for providing lab facilities and we are extremely grateful to Dr. J. A. R. P. Sarma, GVK Biosciences for providing NOC to process part of my research in their lab.

References:

- [1] Tremblay, J, Gerrer, R, Hamet, P., *Adv, Second Messenger Phosphoprotein Res.* 1988, 22, 319 – 383.
- [2] Waldman, M, Murad, F., *Pharmacol. Tev.* 1987, 39, 163 – 196.
- [3] Beavo, J.A, Reifsynyder, D. H., *Trends Pharmacol. Sci.* 1990, 11, 150 – 155.
- [4] Nicholson. C, Challis, R, Shakio, M., *Trends Pharmacol. Sci.* 1991, 12, 19 – 27.
- [5] Helmut Haning, Ulrich Niewo Hner , and Erwin Bischoff., *Phosphodiesterase Type 5 (PDE5) Inhibitors.*, Bayer AG Pharmaceutical Business Group, Medicinal Chemistry, D-42096 Wuppertal, Germany 2 Bayer AG Pharmaceutical Business Group, Institute of Cardiovascular Research II, P.O. Box 101709, D-42096, Wuppertal, Germany.
- [6] Boolell M, Allen MJ, Ballard SA, et al., *Int J Impt Res.* 1996, 8, 47 – 52.
- [7] Wallis RM, Corbin JD, Francis SH, et al., *Am J Cardiol.* 1999, 83, 3C – 12C.
- [8] Goldstein I, Lue TF, Padma-Nathan H, et al., *N Engl J med.* 1998, 338, 1397 – 1404
- [9] G. M. Morris, D. S. Goodsell, R. Huey, and A. J. Olson., *J. Comput.-Aided Mol. Des.* 10, 293, 1996 .
- [10] Cerius 2 Aprogram Suite for Molecular Modelling Activities;Molecular Simulations: Scranton Raod,San Diego,CA 92121 - 752,USA.
- [11] Stewart, J. J. S. J., *Comput.-Aided Mol.Des.*1990, 4, 1.
- [12] Dewar, M. J. S.; Zoebish, E.G.; Healy,E. F.; Stewart, J. J. P. J., *Am.Chem.Soc.*1985 ,107 ,3902.
- [13] Mathew Hahn., *J. Med. Chem.* 1995, 38, 2080-2090
- [14] Mathew Hahn and David Rogers., *J . Med. Chem.* 1995, 38, 2091-2102.
- [15] Pharmacophore Perception, Development and Use in Drug Design; O.F., Ed.; International University Line: La Jolla, CA 2000.
- [16] Brooks, B. R.; Bruccoleri, R. E.; Olafson, B. D.; Sates, D. J.; Swaninathan, S.; Karplus, M. CHAMM., *J. Comput. Chem.* 1983, 4, 187-217.
- [17] Martin, Y. C.,*American Chemical Society, Washington, DC*, 1998; pp 121-148.
- [18] Clark, D. E.; Westhead, D. R.; Sykes, R. A.; Murray, C. W., *J. Comput. Aided Mol. Des.* 1996, 10, 397-416.
- [19] Doweiko, A. M., *J. Med. Chem.* 1994, 37, 1769-1778.
- [20] Mason, J. S.; Good, A. C.; Martin, E. J., *Curr. Pharm. Des.* 2001, 7, 567-597.
- [21] Milne, G. W.; Nicklaus, M. C.; Wang, S., *SAR QSAR Environ. Res.* 1998, 9, 23 -38.
- [22] Catalyst, version 4.6; Accelrys, Inc. (previously known as Molecular Simulations, Inc.): 9685 Scranton Road, San Diego, CA 92121, 2000.
- [23] Sprague, P. W. *Automated chemical hypothesis generation and database searching with Catalyst. In Perspectives in Drug Discovery and Design*, Muller, K., Eds.; ESCOM Science Publishers. B. V.: Leiden, The Netherlands, 1995; pp 1-21.
- [24] Kurogi, Y.; Gu' ner, O. F., *Curr. Med. Chem.* 2001, 8, 1035 1055.
- [25] C.M. Venkatachalam , X. Jiang, T. Oldfield, M. Waldman Accelrys Inc., *Journal of Molecular Graphics and Modelling.* 21 (2003) 289–307
- [26] J.A.R.P.Sarma, G.Rambabu, K.Srikanth, D.Raveendra and M.Vithal., *Bioorganic & Medicinal Chemistry Letters.* 12 (2002) 2689 – 693.

- [27] Gautam R. Desiraju, Bulusu Gopalakrishnan, Ram K. R. Jetti, Dayam Raveendra, Jagarlapudi A. R. P. Sarma and Hosahalli S. Subramanya., *Molecules*. 2000, 5, 945-955.
- [28] Remy Hoffmann and David Kitson - *3D-QSAR Models for ETA Endothelin Antagonists using Catalyst and Cerius2*, Accelrys. http://www.accelrys.com/reference/cases/studies/endothelin_full.html
- [29] Eric A. Jamois, Ph.D. - *Analysis of Multiple QSAR Models - Unleashing the Power of GFA*. http://www.accelrys.com/reference/cases/studies/gfa_qsar.html.